International Conference on Space Optics—ICSO 1997

Toulouse, France

2–4 December 1997

Edited by George Otrio

GAIA: direct fringe detection

E.Thomas, S. Robbe, T. Viard, D. Segransan, D. Dantes, et al.

International Conference on Space Optics — ICSO 1997, edited by Georges Otrio, Proc. of SPIE Vol. 10570, 105700T · © 1997 ESA and CNES · CCC code: 0277-786X/18/$18 · doi: 10.1117/12.2326467

GAIA : DIRECT FRINGE DETECTION

E. THOMAS[1,2], S. ROBBE[1,2], T. VIARD[1], D. SEGRANSAN[2],
D. DANTES[1], F. VAKILI[2], R. KRAWCZYK[1]

Aerospatiale, Future Instruments, 100 Bd du Midi BP 99, 06322 Cannes la Bocca Cdx, France
[2] Observatoire de la Côte d'Azur, Fresnel Department
UMR 6528, Av. Copernic, 06130 Grasse, France
Observatoire de Grenoble, Laboratoire d'Astrophysique, 414 rue de la Piscine, Domaine Universitaire St Martin d'Hères BP 53, 38041 Grenoble Cdx 9, France

ABSTRACT. *The Global Astrometric Interferometer for Astrophysics (GAIA) is a space mission concept featuring several Fizeau interferometers dedicated to wide-angle astrometry and aiming at dramatically increasing the accuracy of angular measurements with respect to Hipparcos (ESA Symposium, Venice, 1997)*
An optical configuration allowing direct fringe detection is presented. It features focal length of 30 m inducing technologically feasible pixel sizes in the bandwidth of interest, and meeting the condition to be included in the ArianeV fairing. The study concerning the configuration is presented in terms of optical and focal plane assembly analyses : feasibility, optical tolerances and performance.

1. INTRODUCTION

The success of Hipparcos (Mignard, 1995) demonstrated the feasibility of obtaining astrometric measurements in space with high accuracy. The result is the construction of the catalogue with 120 000 stars up to about 12 visual magnitude (Perryman, 1997)
The GAIA (Global Astrometric Interferometer for Astrophysics) mission, proposed for a future ESA cornerstone mission, is a successor of Hipparcos. Its goal is to allow additional observations with still better astrometric accuracy and higher limited magnitude.
GAIA has to perform multi-spectral (in six bands) and multi-epoch photometry. The mission length is scheduled for 5 years, justified not only to reach the desired accuracy but also to perform specific astrophysics studies (Perryman & Lindegren, 1995b).
The initial optical configuration was proposed by Perryman & Lindegren (1995a) and optically analysed by Loiseau & Shaklan (1995). The entrance pupil diameter is 0.55 m, the baselength 2.45 m, and the equivalent focal length 11.55 m. The latter, combined with a 1 deg field of view leads to a 20× 20 cm² focal plane. In this configuration, the interfringe is 2.6 µm and the Airy disk size 28 µm, inducing pixel size of 1.3 × 28 µm² (Shannon criterion) not at present technologically achievable. A solution was proposed for the fringe detection consisting in dividing the whole field of view in several subfields and linking each of them with a modulating grid. The observation is performed in a pupil plane. The spatial modulation (interference fringes) is transformed into a temporal modulation detected on a mono-pixel detector. The main drawback is the confusion effect : the intensities coming from each star present in a subfield are integrated without distinction. Thomas (1996) showed the importance to consider this effect on the signal in order to achieve a 10 µas accuracy independently on the visual magnitude and on the galactic latitude of observation.

To compensate for the confusion effect, we propose a new optical configuration which would allow to directly observe in the image focal plane (direct fringe detection), taking into account the expected state-of-the-art CCD technologies described hereafter.

2. OPTICAL CONFIGURATION FOR DIRECT FRINGE DETECTION

2. 1. Requirements

2. 1. 1. Field of view requirements

The major requirements which can be derived in order to specify optical configurations of GAIA come from the astrometric accuracy and the limiting magnitude of the science objects to be observed by the instrument.
The following equations provide the analytical relationships between the various contributing parameters.

The star location accuracy σ depends on the baseline B of the interferometer, the wavelength λ and the Signal to Noise Ratio SNR :

$$\sigma = \frac{\lambda}{2.\pi.B.SNR} \tag{2.1}$$

From the desired value of σ, the required number of photons can be derived. Assuming the other parameters to be known, the integration time τ can be estimated. From τ and from the known mission length L, the required field of view Ω (in str) can be derived from :

$$\Omega = \frac{4.\pi.\tau}{L} \tag{2.2}$$

Considering an instrument of focal length f, the linear dimension dim of the focal plane is given by :

$$\mathrm{dim} = \Omega.f \tag{2.3}$$

The fringe width i can be estimated from the following equation :

$$i = \frac{\lambda.f}{B} \tag{2.4}$$

From Eqs. (2.1) to (2.3), it can be shown that the requirement to achieve 10 μas accuracy for a 15 visual magnitude star dimensions the field of view (FOV) of each interferometer.

This requirement is not the only one to be taken into consideration in specifying the FOV of each interferometer. The required sky coverage, and, in particular, the partial overlap between the sky strips covered by the FOV along successively scanned great circles, will be achieved only if the across-scan dimension of the FOV is larger than a given value. This value depends on the angular separation between two great circles which, in turn, depends on the spin rate ω of the spacecraft, the solar aspect angle ξ, and the precession velocity Vp of the spin axes. Values can be attributed to the two first quantities, i.e. 120 as/s for the spin velocity and 55° for the solar aspect angle (Lindegren & Perryman, 1995). For the precession velocity, we can use the corresponding one from the Hipparcos scanning law, i.e. 6.4 revolutions per year. Given these values, it is possible to derive the displacement of the spin axis Ds, after one revolution :

$$Ds = \mathrm{acos}(\sin(\xi)^2 \cos(\omega.\Delta t) + \cos(\xi)^2) \tag{2.5}$$

where Δt is the necessary time for the satellite to make one rotation.
In order to achieve subsequent scan partial superimposition, the across-scan dimension of the field of view will have to be greater than Ds. From the given values, we obtain $Ds \sim 0.7°$, so a value of 0.8° is considered for the across-scan dimension of the field of view.

2. 1. 2. Focal plane requirements

The requirements on the focal plane are also derived from the mission requirements. Mainly, the limiting magnitude and the brighter stars define the electronic dynamic range requirements of the

pixels. The spin rate of the spacecraft defines the velocity of the fringe motion on the focal plane, whereas the instantaneous integration time directly depends on this parameter. In this section, the considered requirements are integration time and number of Time Delay Integration (TDI) lines.

The instantaneous integration time T is derived from the along-scan size Δx of the pixel and the fringe motion v. The parameter v depends on the spin rate ω of the satellite given in rad/s and on the focal length f of the interferometer given in metres. T is then given by :

$$T = \frac{\Delta x}{v} = \frac{\Delta x}{f.\omega} \qquad (2.6)$$

The number of TDI lines required to obtain an acceptable Signal to Noise Ratio (SNR) value can also be estimated. If RON is the read out noise of the CCD, the required number of photo-electrons can be calculated from :

$$Np = \frac{SNR^2 + \sqrt{SNR^4 + 4.RON^2.SNR^2}}{2} \qquad (2.7)$$

Given Ns, the total number of photo-electrons coming from the star, and producing a given fringe pattern, we can assume that the central fringe contains 20% of this number. Hence, if the number of pixels per fringe is given by P, a pixel in the central fringe collects :

$$Nc = \frac{0.2.Ns}{P} \qquad \text{photo-electrons} \qquad (2.8)$$

The required number of TDI lines is then given by :

$$TDI = \frac{Np}{Nc} \qquad (2.9)$$

The availability of suitable detectors for fringe detection (in the case of direct or indirect detection, visible or infrared) has to be considered, in terms of :

- pixel size : rectangular pixels with 2.4-µm size in the scan direction seem to be achievable according to CCD Philips Imaging Technology's expertise (Peek et al., 1993; Peek et al., 1996)
- sampling resolution : a minimum of about 3 pixels per fringe period seems to be sufficient to provide nearly theoretical performance for the fringe location process
- achievable quantum efficiency
- focal plane dimensions : it is considered reasonable not to exceed some tens of centimetres in linear size, typically 40 cm

Taking into account the scanning velocity of the satellite, the available integration time for a 2.4 µm detector is 133 µs at the most. The number of TDI steps compatible with the required signal to noise ratio ($SNR > 3$), for a star of magnitude 15, is then about 1 500 (with the hypothesis of a 5 e- noise level, see Sect. 2.3.1).

2. 1. 3. Telescope accommodation requirements

The volume of each telescope (in terms of diameter and height of its envelope) is constrained by the internal dimensions of Ariane V Speltra fairing (∅ = 4 570 mm, h = 4 850 mm for the cylindrical section) and by the number of instruments to be accommodated on the Payload Module (PLM). Assuming for the service module a height of 1700 mm, the PLM height cannot exceed about 3 000 mm (cylindrical section only). This limits the height available to each instrument (three have to be stacked on top of each other). An initial value for each interferometer is about 700 mm (internal height of the telescope compartment). This leaves enough room for the accommodation of an additional instrument, ARVI (Auxiliary Radial-Velocity Instrument) dedicated to radial velocity measurements (Favata & Perryman, 1997), for which, however, the non-cylindrical upper region of the Speltra could be exploited (Fig. 1). The Speltra also limits the

diameter of each interferometer. Considering a reasonable thickness of the PLM wall and its thermal cover, the maximum allowable diameter for each interferometer will be about 4.2-4.3 m. Inside the PLM, each telescope shall be mounted with its baseline vector orthogonal to the nominal spin axis of the spacecraft, and with the line of sight oriented according to the values defined for the basic line-of-sight angles ($\gamma_1 = 54°$, $\gamma_2 = 78.5°$, $\gamma_3 = 132.5°$ have been proposed for the three-telescope configuration). The mounting tolerances have to be defined within the alignment budget that has to be set up.

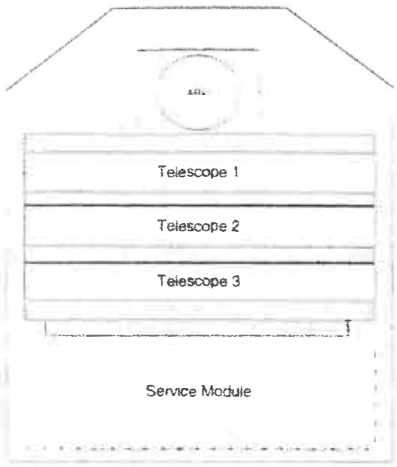

Fig. 1 Telescope accommodation in the Speltra

2. 1. 4. Calibration and stability requirements

Calibration of residual aberrations has to be performed taking into account the required value of fringe contrast and displacement of the Airy disk centroid, over the whole field of view. Particular attention is paid to distortion introduced by the optical design, as its level must be compatible with a single TDI clocking rate applicable throughout the FOV (or, at least to a single CCD chip).

The requirements on opto-mechanical tolerances, in terms of tilt and decenterings, have to be given for each mirror, in order to reach the desired performance in terms of Airy disk location estimation. An instantaneous astrometric accuracy of 100 µas is required in order to achieve the final 10 µas accuracy on the measurements. Considering the 30-m focal length, this accuracy can be achieved if the centroid displacement induced by spurious effects is less than 15 nm.

An algorithm dedicated to fringe contrast computation, based on Zernike polynomials derived from CodeV calculations, has been developed by Aerospatiale. Requirements on opto-mechanical tolerances are computed from CodeV results.

2. 2. Optical configuration description

The linear pixel dimension along TDI scanning direction is related to the interferometer parameters, baseline B, focal length f, and wavelength of observation λ (Eq. 2.4.).
Considering an achievable pixel size a equal to 2.4 µm, a baseline B of 2.55 m, and an instrument focal length of 30 m, we obtain 2.7 pixels per fringe at 0.55 µm, which is a reasonable value to achieve theoretical performance for the fringe location process.
The scheme of the proposed optical configuration is shown on Fig. 2.

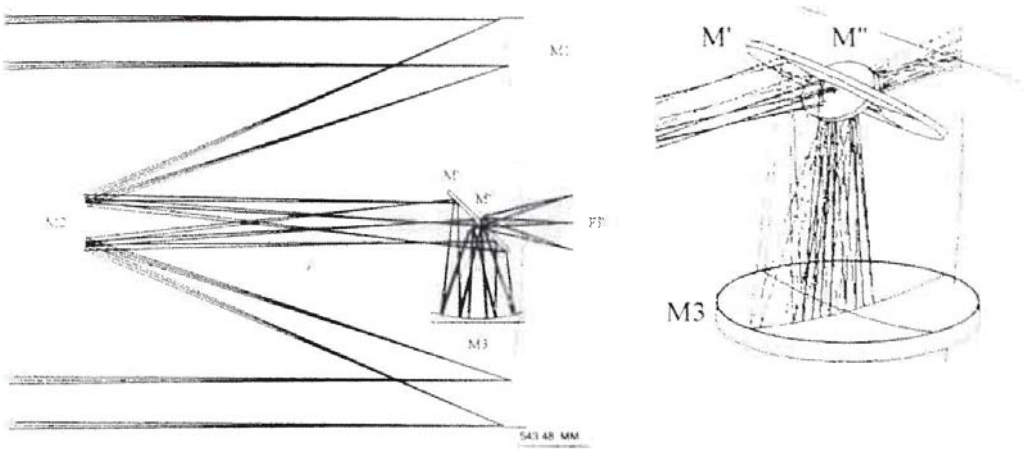

Fig. 2 Korsch configuration and associated relay system

This configuration is a Korsch one, composed of three aspherical mirrors (M1, M2 and M3). It allows the formation of a real exit pupil, simplifying the possible insertion of active optics and of baffling.

To take into account dimensions of the ArianeV envelope and space dedicated to structure and mechanics, an optical relay system is implemented to fold the light beam in another direction. This relay system is the combination of two flat mirrors (M' and M"), as shown on Fig. 2.

The obstruction percentage of the field of view due to the optical relay system is about 0.15%.

Table 1 gives the optical parameters of the configuration, in terms of radius of curvature of the mirrors, conical constants and the distance of the mirrors to the following surface. The characteristics of the optical layout (focal length, baseline, aperture's diameter, etc...) is given in Table 2. The spot diagrams given by the optical tool CodeV using two 60 cm apertures are given on Fig. 3.

Table 1 Optical parameters of the Korsch configuration

Surface	Radius of curvature (mm)	Conical constant	4th and 6th order terms	Distance to the following surface (mm)
M1	-7654.49	-0.991257	-0.1217E-14 0.6098E-24	-3370.42
M2	-1103.27	-1.787285	0.3104E-11 -0.1686E-17	3017.73
M'	∞	-	-	--747.02
M3	1270.36	-1.502707	0.5435E-10 -0.2524E-17	747.02
M"	∞	-	-	-743.86
FP		-	-	0.0152

Table 2 Characteristics of the Korsch configuration

Effective focal length	30 m
Baseline	2.55 m
Aperture's diameter	600 mm
Square field of view	$0.8° \times 0.8°$
Focal plane dimensions	42 cm × 42 cm
Diffraction-limited circular FOV	1.1° diameter
Number of reflections	5 (3 aspherical and 2 flat mirrors)
Fringe width	6.5 µm at λ = 550 nm
Airy disk size	about 70 µm at λ = 550 nm
number of 2.4µm-pixels per fringe	2.7 pixels at λ = 550 nm
Total pixel number (2.4µm × 67µm)	175 000×6 270

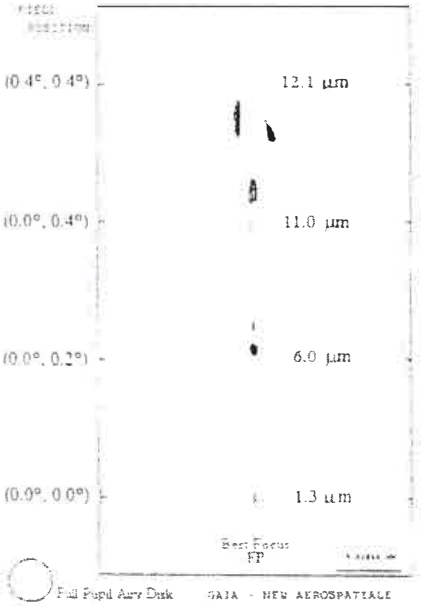

Fig. 3 Interferometric spot diagrams for the Korsch configuration

2. 3. Focal Plane Assembly configuration from Philips Imaging Technology

2. 3. 1. Performance of detector technology

Philips technology offers very small pixel size (2.4 µm) and also very large 2D arrays. This is made possible with the use of a specific technique called building block concept or stitching. During the stitching process, which is performed in clean room, the wafer is moved with an accuracy of 0.15 µm and it is possible to combine elementary blocks and to manufacture a CCD whose size is only limited by the size of the wafers and by the position of the alignment markers. The maximum size for a CCD module should be 88 mm x 110 mm with the existing tools in Philips. This can allow to constitute the complete 2D detector array with 4 x 5 modules of this size.

However, an optimisation of this module size has to be performed, taking into account the number of dices per water, the yields, and the associated costs which increase very fast with the module size

A sensitivity of 30 % is possible at 550 nm. For larger wavelengths, simulations would be required with specific pixel sizes in order to estimate the sensitivity.

A requirement of 60 000e- for the charge handling capacity was taken as a baseline for our application For a conventional detector, this capacity depends a lot on the resistivity of the substrate, which is usually 5 Ωcm or 30 Ωcm . The electron density depends of course on the pixel size. For sizes around 10 µm, the density is between 500 e-/µm^2 and 800 e-/µm^2, depending on the sensitivity of the substrate. For Philips pixel size of 2.4x2.4 µm , a performance of 14 000 electrons is achieved. The value of 60 000 e- seems to be achievable for a 2.4x70 µm pixel, 70 µm being the estimated Airy disk size.

Charge transfer efficiency (CTE) can be a very critical point for a CCD operating in TDI mode. The requirement in CTE is related to the number of TDI lines. If the number of lines is small, a high value of CTE can be acceptable (typically 10^{-3}). For this application, a large number of TDI lines may be required (1 500 lines as derived in Sect. 2.1.2.). A CTE of 10 may be required in order to reduce the noise level at the output of the detector. For the brightest stars, which are not the most critical, the CTE is the most limiting factor, due to the large number of charge transfers. This value seems to be compatible with the technology existing in Philips.

Dark current has to be taken into account for detectors using long integration time, which is the case for TDI with a large number of lines. The dark current obtained from Philips detectors is very small compared to that from other technologies, and can nearly be compared with detectors operating in Multi Pinned Phase (MPP) mode , even if this mode does not bring significant interest in the case of Philips technology. Dark current can be lower than 0.5 nA/cm2 at 60°C.
On a first approach, it seems that the dark current obtained at -50 °C should be compatible with the required performance, considering the used number of TDI lines.

The level of noise which can be foreseen for such detectors should not be very different from conventional CCDs. The noise mechanism is very similar. The noise at the detector output should be around 100 µV rms if we assume an optimised detector. A conversion factor of 20 µV/e- seems achievable with Philips technology, which corresponds to a noise level of 5 e-. This noise level can however be considered as a critical point.

The technical alternatives to obtain 40 cm long detector is to use an interconnection substrate to arrange modules to constitute the whole detector. The type of substrate and the butting mode have completely to be defined : materials compatible with silicon, ceramic, kovar, AlN, materials with wettable surfaces in order to correctly align the different modules. The most critical alignment is certainly the performance in the plane of the substrate. The performance in the direction orthogonal to the plane should not be very critical. The electrical connection aspects have to be addressed and influence the size of the dead zones between modules. The flatness performance is related to the choice of the substrate/packaging. The contribution of the CCD modules is very small.

The MTF performance described in Philips papers (Peek et al., 1996) shows very high values (0.64 at Nyquist frequencies for 2.4 µm pixels) which certainly take into account the effect of dead zones between pixels and which improve artificially the MTF. Nevertheless, the MTF performance does not seem to be a critical point.

Considering the TDI requirement (Sect. 2.1.2.), it is important to record a larger number of independent samples from each star (Gay & Lattanzi, private communication). Several configurations were proposed, and the one retained is that referred to as "chip tilt", in which the detector is positioned with a small inclination angle with respect to the scanning direction, by virtue of which, after 1 500 TDI steps, the diffraction patterns passes from one TDI column to another. With this configuration, the number of independent samples of a given diffraction pattern are dependent on the focal plane size and the number of pixels in the scanning direction. As it is important to maximise the number of samples, we assume a FOV requirement of about 0.8° in the scanning direction, corresponding to a focal plane size of approximately 42 cm.

It is then possible to summarise the characteristics related to the format of the detector:

- overall size: 42 cm x 42 cm
- pixel size: 2.4 µm x 70 µm
- number of pixels in the across-scan direction: about 6 270 (taking into account detector manufacturing constraints)
- number of pixels in the along-scan direction: about 175 000 (taking into account detector manufacturing constraints)
- number of chips : 4 x 5 with a size of 88 x110 mm²

The detector capacitance of 60 000e- is compatible with 7-magnitude stars. From 6 and for lower values, the pixels saturate and an antiblooming drain should be implemented in order not to saturate the neighbouring pixels. A 0-magnitude star corresponds to a level of signal which is more than 400 times the saturation level of 60 000 e-. The technology used by Philips Imaging is very different from those classically used in the space applications. The superimposition of a N substrate, a P well layer and a N well constitutes a natural and vertical antiblooming device. The level of saturation foreseen here seems compatible with the levels already demonstrated for broadcast and medical applications.
For 15-magnitude stars, the signal on the central pixel becomes very small : about 25 e- on the central pixels, which corresponds to voltages of 500 µV.

2. 3. 2. Data rate

The choice has been made here to restrict the frequency of each video chain to not more than 3 Msamples per second. In the case of the MERIS program (ESA / Envisat), the performance of the video chain is 1 Msps with a resolution of 12 bits, the best achieved in today's space applications. For GAIA, a performance of 3 Msps/12 bits could be achieved with a reasonable technological effort, and this value can be taken as a preliminary baseline. Nevertheless, some feedback has to be sought from video chain manufacturers in order to verify the feasibility of a 6 Msps/12 bits implementation compatible with the GAIA planning.
Taking the baseline value given above and the line period of 133 µs, 4 outputs would be needed per chip : each CCD output would then read out 392 pixels (this is a preliminary value). For the whole focal plane, 80 video chains must operate in parallel in order to amplify, filter, clamp and digitally convert the video signals of one telescope. It should be pointed out that with 6 Msps video chains, the number of chains would be 40 for each telescope, a number comparable with existing space applications currently under development in Aerospatiale.

The exact video frequency will be 2.9 Msps. The total rate for 80 video chains and after the 12-bit conversion is 2.8 Gbits per second. This data rate, together with the number of parallel video chains may be considered as very high and critical.
In addition to the critical budgets of the APU (Analogical Processing Unit), this very high data rate leads to the problem of oversizing the memory units and the specification of a raw data rate of

50 Mbps at the output of the payload would seem far too limiting. Two solutions may be identified to reduce this value : data reduction and data compression.

2. 3. 3. Data reduction

Two main factors (Gay & Lattanzi, private communications) could theoretically allow a reduction in the PLM output data rate

- Over the whole mission, it can be expected that an average of only 3% of the temporal lines provided by a CCD will contain the fringes of a star equal or brighter in magnitude than $m_V = 15$. Towards the centre of the galactic plane, where the mean density of stars ($m_V \leq 15$) is much higher, the local ratio of useful lines could be on average as high as 25%, and locally much higher.
- For a given *useful* temporal line (having a mean number of 10 targets), it can be shown that, on average, only half of the pixels contain useful information (i.e. star fringes of interest).

The first factor does not reduce the data rate at the output of the APU. For each line, the 392 pixels at the 80 CCD outputs would still have to be read out in 133 µs. It is of no help to insert zeros instead of dark pixels.

On the other hand, at the input to the digital processing chain, it would certainly be possible to calculate in real time the average value for each line stored in a buffer, and to decide whether or not to move it to the mass memory, according to the number of identified targets and their respective brightness. The suppression task could be made even more straightforward if an on-board catalogue allowed *a priori* identification of non-useful lines. In the case of observations near the galactic plane, it seems likely that the *a priori* selection would be needed in order to keep the data rate to an acceptable level (otherwise, in some regions of the galactic centre, some tens of thousands of ≤ 15th magnitude stars could be identified within a single square degree of field). Taking into account this potential suppression of CCD lines, the data rate at the output of the APU (for one interferometer) limited to 2.8 Gbps, would reach at the most, 700 Mbps at the output of the Digital Processing Unit (DPU). This approach would thus enable a significant reduction to be achieved in mass memory requirements. In the mean case (i.e. assuming on average only 3% of the lines to contain useful information), the DPU output frequency would be reduced to 84 Mbps.

The second of the above-stated approaches could also be considered as a potential means of reducing the data rate at the detector output : following discussions with detector manufacturers, it seems possible to read and dump non-useful pixels at a very high rate, and to read the useful ones out more slowly, multiplying by two the frequency line in the most optimistic case. This would allow the number of CCD outputs and video chain units to be reduced, around 40 outputs would be needed, each associated with 784 physical pixels per CCD line, of which about 392 (half) would need to be read out. This procedure would require the use of an on-board catalogue containing previously known star positions, together with Star Tracker information provided by the Service Module, in order to predictively identify the pixels to be read out for each temporal line, and to program the detector clocks accordingly for the whole readout sequence.

The advantages and drawbacks of implementing the above-described data reduction technique, at the CCD output must be analysed.
If this approach is not, or cannot be implemented at detector level, it could still be possible to do it in the DPU. Each pixel of a new line would be stored in a buffer at the DPU input, and would not be moved to the mass memory if its signal were not higher than some predetermined level.

By combining the potential effects of the above two data "suppression" techniques, it could be expected that the maximum data rate at the output of the DPU would be reduced to around 350 Mbps (worst case), whereas the mean rate would be 42 Mbps.

2. 3. 4. Data compression

To meet the anticipated down-link data flow requirements of GAIA, an appropriate data compression technique will need to be implemented.
The challenge of the compression technique is to ensure that the information relevant to the star fringe position (phase) information is adequately represented. It will be important to ensure either full recovery of the original data, or to tolerate an "acceptable" level of data degradation. Algorithms referred to as "lossless" provide compression without any loss of information, as opposed to "quasi-lossless" algorithms which belong to the lossy or non reversible category, where a fraction of information is irretrievably lost during compression. Quality criteria are needed to assess whether or not the degradation of a quasi-lossless algorithm can be accepted.
Therefore, system requirements must take into account the performance regime of the compression module and, consequently, the requirements of any compression technique should be split into different aspects, namely

- Image quality : application oriented, data quality criteria
  data quality degradation
- Compression ratio : performance of the algorithm in terms of data rate compression
- On board implementation : complexity of the electronic architecture
  - quantisation / encoding function flexibility

The compression performance also depends on the characteristics of the data being compressed, and in particular on the redundancies in its content.

Background experience in spectral imagery shows that a single panchromatic or spectral band can be approximately losslessly compressed by a ratio of 2, whereas multidimensional algorithms operating in both spatial and additional dimensions (i.e. temporal, optical wavelength,...) can reach higher compression ratios at the expense of simplicity. In the context of the direct detection of stellar fringe patterns with GAIA, the use of Fourier or wavelet analysis could conceivably enable repetitive or semi-redundant information content to be discarded. The extensive exploitation of statistical redundancies can also improve the achievable compression ratios. Factors in favour of this option are

- cost in implementing on board data compression is necessarily that of added complexity within the architecture and the processing chain of the data handling system
- *a posteriori* analysis of the transmitted data content could enable engineers to devise improved compression strategies, once GAIA has been launched, and for this reason the on-board hardware should be designed to enable new algorithms to be uploaded

2. 4. Proposed structure design

The proposed structure design is one example among other ones to illustrate the design possibility of such optics system.
The structural concept is driven by stiffness and strength to reduce mass :

- The M1 and M2 mirrors are linked together via a structure made of beams and on the basis of an undeformable triangle shape.
- In the middle and on the side of M2 mirrors, internal shear walls are located. They allow a reduction of the length of this structure in order to avoid general buckling, to transfer loads to the external structure which closes the optical cavity, and to transfer loads between modules through an external cylindrical shell. The shear wall is also used to support the M2 subsystem.

- The flat mirrors are also fixed through a beam structure and a share wall linked to the main wall.
- The focal plane is fixed through beams directly to the M2 subsystem interface point, to avoid instability that could occur with complicated mechanical load paths.
- To avoid straylight, different lightweight baffles are fixed to the structure. We have two main baffles at the entrance of the optical cavity, and a pupil baffle near the flat mirror.

The proposed concept is illustrated on Fig. 4.

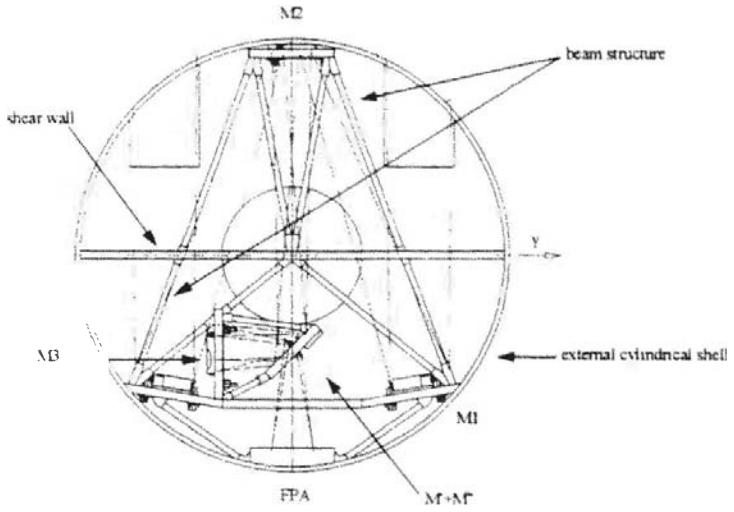

Fig. 4 Proposed structural concept for GAIA

3. PERFORMANCE : OPTICAL QUALITY AND SENSITIVITY

3. 1. Korsch configuration optical quality

3. 1. 1. Presentation of the Software for Interferometer Visibility Analysis

We developed an algorithm, named SIVA for Software for Interferometer Visibility Analysis, dedicated to assess the performance of optical configurations for 2-telescope interferometer. The two identified criteria to evaluate the optical quality are

- fringe contrast
- displacement of the Airy disk

SIVA estimates the fringe contrast from the wavefront decomposition in Zernike polynomials. The coefficients of the Zernike polynomials are given by CodeV which calculates them for different points in the field of view once the optical configuration has been integrated.

3. 1. 2. Results

SIVA uses the outputs of CodeV (Zernike polynomial coefficients) to estimate fringe contrast and Airy disk displacement as a function of points in the field of view.
Figure 5 shows an example of the contrast estimate and Airy disk displacement for two different points : centre of the field of view and field edge. The hypotheses are :

- pupil diameter : 60 cm
- baselength : 2.55 m
- wavelength : 550 nm
- Field of view : 0.8×0.8 deg^2

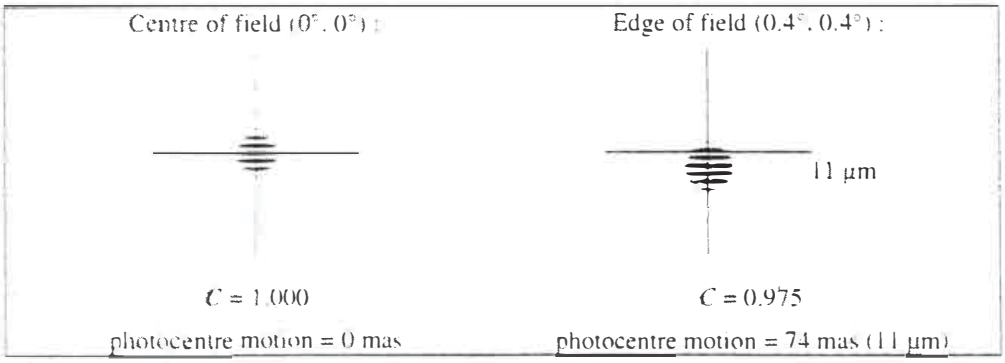

Fig. 5 Visualisation of fringe patterns, contrast and Airy disk centroid displacement computation.

SIVA was validated by comparison with CodeV results in terms of calculation of the Modulation Transfer Function, and real and imaginary parts of the Optical Transfer Function.
Table 3 shows the estimated contrast and centroid displacement for different points in the field of view of the Korsch configuration. The focal length varies in the field due to the distortion. This has to be taken into account in the centroid location estimations.

Table 3 Contrast and centroid displacement estimated for different points in the field of view

FOV	**1 : (0.0°, 0.0°)**	**2 : (0.0°, 0.2°)**	**3 : (0.0°, 0.4°)**	**4 : (0.4°, 0.4°)**
Contrast	0.998	0.995	0.991	0.975
Centroid displacement	0 mas 0 µm	52.5 mas 8 µm	3.5 mas 0.5 µm	73.6 mas 11 µm

The contrast remains high in the whole field (> 95%). There is a displacement of the chief ray, 8 µm and 11 µm respectively at the (0.0°,0.2°) and (0.4°,0.4°) points, which has to be taken into account for data calibration.

3. 2. Korsch configuration sensitivity

We performed analyses of the Korsch configuration to assess its performance in terms of sensitivity to misalignments. This sensitivity is expressed by the centroid displacement, more severe than visibility criterion, induced by a tilt or decentering of one mirror.

An instantaneous astrometric accuracy of 100 µas is required in order to achieve the final 10 µas accuracy on the measurements. Considering the 30-m focal length, this accuracy can be achieved if the centroid displacement induced by spurious effects is less than 15 nm. The misalignments we analyse here are the followings :

- $\Delta\alpha$: tilt around the x-axis (normal to baseline)
- Δy : decentering along the y-axis (parallel to baseline)
- Δz : decentering along the z-axis

These effects are analysed on each aspherical mirror (M1, M2 and M3). The contributions of each mirror misalignment to the astrometric accuracy degradation are assumed to be equivalent. The final centroid displacement is so assumed to be the quadratic sum of the displacements induced by each contribution. So that, the latter must be less than 5 nm.

Figures 6, 7 and 8 show $\Delta\alpha$, Δy, and Δz of each mirror as a function of centroid displacement. Table 4 gives the estimated maximum tilts and decenterings, for which centroid displacements less than 5 nm are maintained. The results show that tolerances require nanometric metrology to control the positions of the mirrors if the astrometric precision must be saved. The control of the primary mirror (M1) seems to be the most stringent, as it requires less than 20-μas tilt and 1-nm decentering. The control of the other mirrors is less constraining.

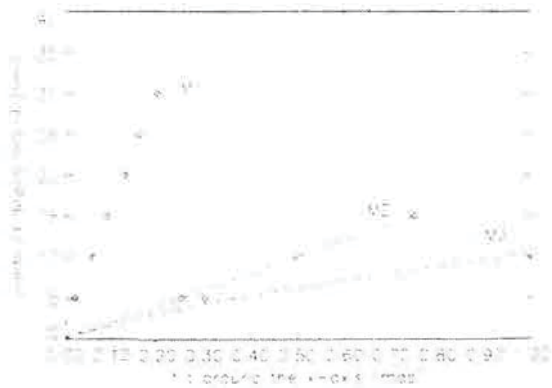

Fig. 6 Centroid displacement as a function of a tilt around the x-axis (normal to baseline) of each aspherical mirror (M1, M2 and M3)

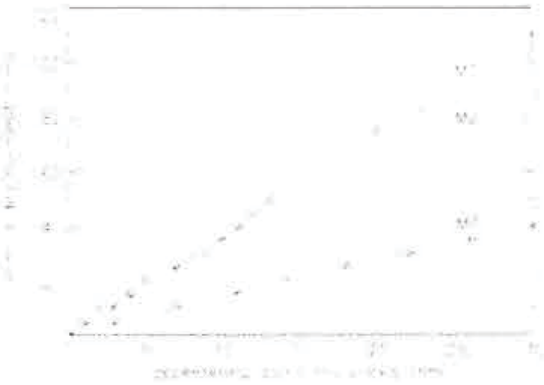

Fig. 7 Centroid displacement as a function of a decentering along the y-axis of each aspherical mirror (M1, M2 and M3)

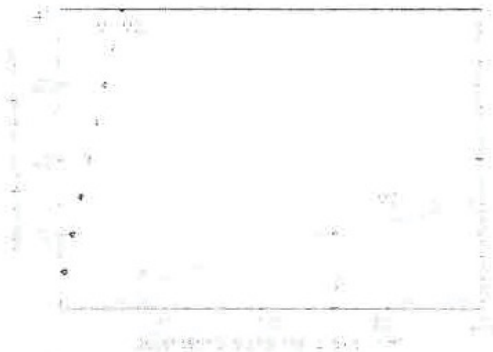

Fig. 8 Centroid displacement as a function of a decentering along the z-axis of each aspherical mirror (M1, M2 and M3)

Table 4 Tolerances of the Korsch configuration

	< 5 nm centroid shift
tilt Δα	
M1	20 μas
M2	250 μas
M3	350 μas
decentering Δy	
M1	1 nm
M2	1 nm
M3	3 nm
decentering Δz	
M1	2 nm
M2	3 nm
M3	40 nm

4. CONCLUSION

A new optical configuration has been proposed for GAIA to allow direct fringe detection. It allows to get rid of the confusion effect present in the initial optical configuration with indirect fringe observation, while considering the expected state-of-the-art CCD technologies and the dimension requirements to fit in the ArianeV fairing.

Based on a pixel size feasibility of 2.4 μm (Philips Imaging Technology), the proposed configuration is a Korsch interferometer with two 0.6-m pupils separated by a baseline of 2.55 m, and with a focal length of 30 m. Its performance in the whole field of view has been assessed in terms of fringe contrast value and centroid displacement. The contrast remains higher than 0.95. However, the centroid displacement due to distortion in the field of view requires data calibration.

The sensitivity of the configuration to misalignments has also been evaluated. Results show that tolerances require nanometric metrology and less than 20-μas tilt to save the astrometric accuracy. The control of the primary mirror is the most stringent.

The characteristics of the associated focal plane are the following :

- overall size: 42 cm x 42 cm
- pixel size: 2.4 μm x 70 μm
- number of pixels in the across-scan direction: about 6 270
- number of pixels in the along-scan direction: about 175 000

Acknowledgements. This work was performed during a study conducted under ALENIA's prime contractorship (in the framework of the APLT-AMTS ESA contract) and the activities were carried out in cooperation with the Observatory of Turino (OATo).

REFERENCES

Favata F., Perryman M.A.C., 1997, Prospects of Microarcsec Astrometry : the Science. In : Battrick B. (ed.) Proc. ESA SP-402, Hipparcos Venice'97, Venice, Italy, 771

Mignard F., 1995, Highlights of the Hipparcos Mission. In : Perryman M.A.C., van Leeuwen F. (eds.) Proc. RGO-ESA SP-379, Future Possibilities for Astrometry in Space, Cambridge, UK, 19

Lindegren L., Perryman M.A.C., 1995, The GAIA Concept. In : Perryman M.A.C., van Leeuwen F. (eds.) Proc. RGO-ESA SP-379, Future Possibilities for Astrometry in Space, Cambridge, UK, 23

Lindegren L., Perryman M.A.C., 1995, Scientific Aspects. In : Perryman M.A.C., van Leeuwen F. (eds.) Proc. RGO-ESA SP-379, Future Possibilities for Astrometry in Space, Cambridge, UK, 35

Lorseau S., Shaklan S., 1996, A&AS, 117, 167

Peek H.L., Theuwissen A.J.P., Kokshoorn A.L., Daemen E.J.M., 1993, In : IEDM Techn. Digest, 567

Peek H.L., Verbugt D.W., Beenhakkers M.J., Huinink W.F., Kleimann A.C., 1996, In : IEDM Techn. Digest, IEDM'96, San Francisco, USA

Perryman M.A.C., 1997, Description of the Hipparcos and Tycho Catalogues. In : Battrick B. (ed.) Proc. ESA SP-402, Hipparcos Venice'97, Venice, Italy, 1

Thomas E., 1996, Evaluation of the Confusion Effect on the GAIA Astrometric Accuracy, AEROSPATIALE Report SE/TNI 318/96